BEAM TESTS OF THE 10 KeV INJECTOR FOR THE UNIVERSITY OF MARYLAND ELECTRON RING (UMER)*

S. Bernal†, H. Li, M. Virgo, S.P. Kwon, M. Holland, R.A. Kishek, A. Valfells, T. Godlove, P.G. O'Shea, M. Reiser and V. Yun, Institute for Research in Electronics and Applied Physics, University of Maryland, College Park, and D. Kehne, FM Technologies, Inc.

Abstract

Results are presented of the first experiments with a 10 keV, 100 mA beam in the matching section for UMER. The section, about 1.5 m long, consists of one short solenoid, six printed-circuit (PC) quadrupoles, a bend PC dipole, a number of steering dipoles, and two sets of Helmholtz coils for balancing the Earth's field. The 2 RMS beam radius as a function of axial distance in the straight part of the beam line is obtained from fluorescent screen pictures. The results are compared with calculations using the K-V envelope equations. The importance of an accurate determination of the initial conditions, i.e. beam envelope size and slope at the entrance plane, as well as the emittance, is emphasized. Furthermore, the role of different types of errors, specially misalignment and quadrupole rotations is discussed.

1 INTRODUCTION

The University of Maryland Electron Ring (UMER) [1, 2] is a model recirculator for studies of space-charge dominated beam transport. UMER has potential applications in many areas ranging from accelerators for high energy physics to spallation neutron sources and heavy-ion fusion drivers. The injector section, which involves elements for matching and deflection into the ring lattice, is a key component of UMER. This paper reports results of the first envelope matching experiments with a 10 keV, 100 mA, 100 ns electron beam. These values represent the nominal beam parameters for UMER. The design and initial development of the injector, including details of the Pierce-type gridded gun and electronics, were presented before [3]. In addition, related matching experiments with a 4 keV, 17 mA, 5 μs electron beam appear in Ref. [4].

2 BEAM LINE AND DIAGNOSTICS

While the final injector, the one intended for multi-turn operation of UMER, requires two pulsed quadrupoles for focusing and one pulsed dipole for deflection [3], the injector described here uses DC elements exclusively. This "DC" injector will function adequately for the first turn and will permit us to understand and refine the design of the pulsed injector and extractor sections. The latter, as illustrated in the general paper on UMER [2], is a replica of the injector section.

The electron gun for the injector is a Pierce-type, cathode-driven gun with a control grid and variable anode-cathode gap [3]. The gun has been tested over several months to find optimal operating points for cathode temperature, anode-cathode gap, grid bias voltage and pulser voltage. With the improved electronics now in use, upper bounds to the beam emittance (4 rms) and energy spread are estimated to be 60 mm mrad and 20 eV, respectively, for a 10 keV, 100 mA beam a few cm downstream from the gun anode aperture. To complement the tests, computer simulations of the gun are presented in an accompanying paper [5].

The focusing channel in the injector consists of six air-core printed-circuit magnetic quadrupoles and one printed-circuit bending dipole. The magnetic fields of these elements have been characterized extensively, as reported in Ref. [6]. The schematics of the DC injector are shown in Fig.1. Figure 2 shows a photograph of the straight section containing the first four quadrupoles. Besides the quadrupoles and main deflecting dipole, four pairs of printed-circuit short dipoles are used as steering elements. Further, a set of long wires in a special configuration act as Helmholtz coils for balancing of the Earth's magnetic field.

The main diagnostics used for experiments in the straight section is a 1.6 cm (diameter) fluorescent screen. The screen can be moved from about 30 cm to more than 1 m out from the aperture plate. A CCD camera with associated hardware for video capture and software for image analysis allows beam profiling along the channel. In turn, the intensity distribution on the fluorescent screen is taken as representative of the electron particle distribution (time-integrated over many beam pulses), so calculations of rms beam sizes are possible. Other diagnostics include a fast beam-position-monitor [7], specially useful in the bend experiments, and a Pearson transformer.

3 ROOT-MEAN-SQUARE ENVELOPE MATCHING

The initial conditions of the electron beam must be accurately determined before realistic calculations of rms envelope matching can be done. The initial beam envelope radius and slope are obtained from a study of beam free expansion over about 15 cm starting at the back of an aperture plate near the electron gun exit. Although the detailed beam expansion depends on the emittance, the initial con-

* Work supported by the U.S. Department of Energy.
† sabern@glue.umd.edu

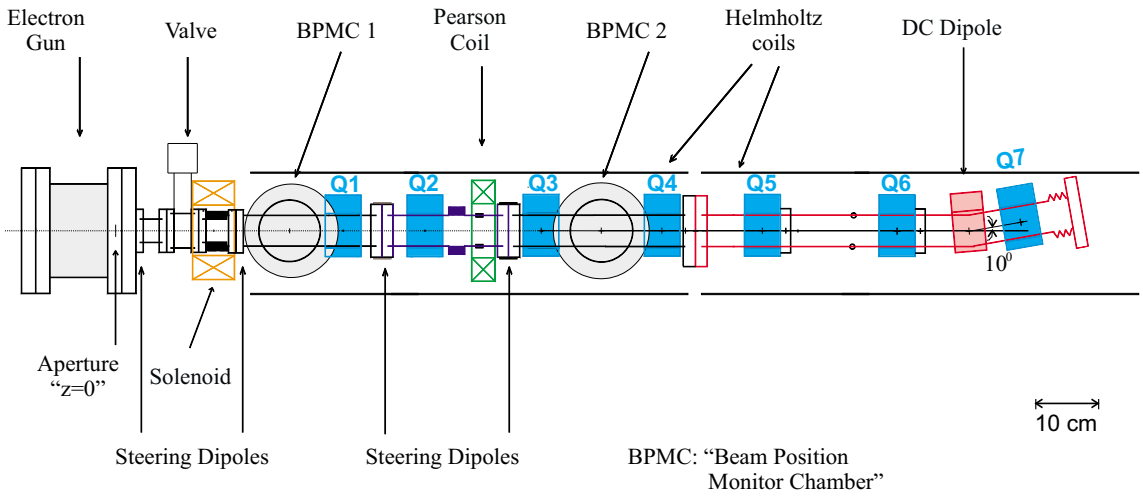

Figure 1: Layout of DC injector for UMER.

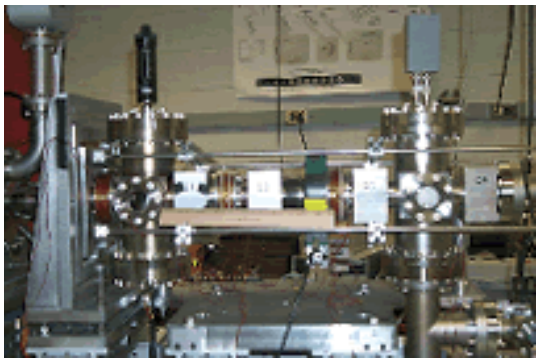

Figure 2: Photo of straight part of injector.

ditions, as obtained from fitting K-V calculations to experimental beam sizes, are relatively insensitive to the exact emittance value. In any case, the emittance was measured with the built-in pepper-pot (1.4 cm from the anode aperture), and the measurements repeated with a second pepper-pot located 48.3 cm from the aperture plate. To check for consistency, the emittance measurements were done for different aperture sizes and beam energies. The expected scaling was found, within measurement errors mostly related to the analysis of pepper-pot pictures. The value quoted in Table I corresponds to our best estimate for a 10 keV, 100 mA beam. This beam is obtained with an anode-cathode gap of 25.35 mm.

Table 1: Beam parameters in UMER injector

Beam Energy	10 keV
Beam Current	100 mA
Generalized perveance	1.5×10^{-3}
4 rms emittance	60 mm mrad
Transport pipe radius	25.4 mm
Initial 2 rms Beam Radius	3.2 mm,
Initial Beam Slope	0.0 mrad

With the initial conditions and other relevant parameters in Table I, the K-V envelope equations are solved for the lattice illustrated in Fig. 1. The strengths of the solenoid and six quadrupoles are varied until an optimized solution is obtained for rms matching into a FODO lattice starting at Q7, right after the 10 degree bend. The K-V envelope computer code SPOT [8] is used for the calculations; the detailed procedure is presented in Ref. [4].

4 RESULTS AND CONCLUSIONS

Table II contains the center locations of elements along the injector section, as well as the solenoid's peak field and quadrupole peak gradients. The locations, dictated by previous matching calculations and by mechanical constrains, are measured from the back plane of an aperture plate near the electron gun exit. The figures for solenoid field and quadrupole gradients, on the other hand, are the result of optimization runs with SPOT for rms matching corresponding to zero-current phase advances of $\sigma_0 = 76^0$, and 85^0 in the FODO lattice of UMER. The negative signs in Table II indicate defocusing in "x", or horizontal direction. Notice that the maximum B field at the edge of a quadrupole is only about 25 G.

Table 2: Parameters for rms matching

Element	**Z(cm)**	$\sigma_0 = 76^0$	$\sigma_0 = 85^0$
Solenoid	16.1	105.2 G	106.7 G
Q1	38.9	6.40 G/cm	6.87 G/cm
Q2	52.3	−8.64	−9.13
Q3	71.2	7.90	8.38
Q4	90.8	−6.91	−7.67
Q5	110.5	7.22	8.04
Q6	133.1	−7.05	−7.85
Q7	152.7	7.80	8.56

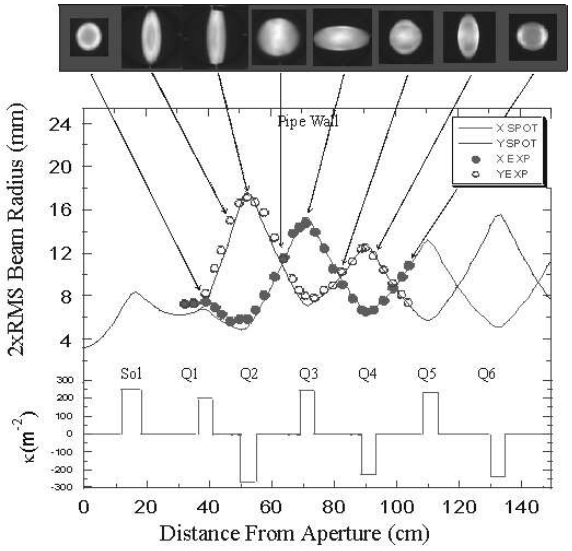

Figure 3: Envelope calculations vs. experiment for $\sigma_0 = 85^0$.

Figure 3 summarizes the results of experiments with a phase advance of $\sigma_0 = 85^0$. The focusing function, $\kappa(z)$, at the bottom of Fig.3 is proportional to the square of the magnetic field (solenoid) or the field gradient (quadrupoles). No adjustment of any experimental parameter within errors was necessary to obtain the excellent agreement shown between experimental beam sizes and envelope calculations. Similar agreement was obtained with $\sigma_0 = 76^0$. The main errors in determining the beam 2 rms radii (about $\pm$ 0.5 mm) arise from picture calibration (i.e. number of pixels per mm in the digitized pictures), and, to a lesser extent, from picture processing (background and noise reductions). Care was taken to avoid saturation of the CCD camera sensor. Since the saturation threshold of the phosphor screen itself (in W/cm^2) is much higher, and the duty cycle for a 100 ns beam pulse at 60 Hz is very small, the effect of screen nonlinearities is not believed to be significant.

Naturally, errors from initial beam misalignment and from quadrupole displacements affect the beam centroid, but not the beam size directly. Only large centroid errors lead to appreciable image forces which increase the errors and distort the beam; however, no errors of such magnitude were present. The center of the phosphor screen was used as the reference for "beam alignment": a combination of Helmholtz coils and steering dipoles was used empirically to force the beam to fall at the center of the screen. However, mechanical imperfections of the phosphor-screen transport system result in a changing phosphor screen center along the focusing channel, relative to the transport pipe axis, of the order of $\pm$ 0.5 mm. Furthermore, by construction, the quadrupole magnetic and mechanical axes coincide within a small fraction of one mm, but may be displaced relative to the pipe axis by as much as 0.5 mm.

Additional errors arise from quadrupole rotations, but are minimized by construction. Quadrupoles Q1 through Q4 (see Fig.1) share a common support plate: the quadrupole halves are clamped to a plate, which is flat to within 0.01 mm. A similar setup is implemented for Q5 through Q7. To better understand the magnitude of these errors, a controlled experiment was designed whose results are presented in a separate paper [9].

Tests with the 10 deg. bend section of the injector are underway. Work in the near future will involve replacing the bend part with a straight section for additional checking of matching conditions, and latter combining the bend and straight extension for a final check. Injection into a number of bend sections in the ring will follow.

5 ACKNOWLEDGMENTS

We thank M. Glanzer and M. Walter for their work with mechanical design and construction, and B. Quinn, N. Rahimi and R. Yun for helpful assistance with the experiments and processing of pictures. This work is supported by the U.S. Department of Energy.

6 REFERENCES

[1] http://www.ireap.umd.edu/umer.

[2] P.G. O'Shea *et al*, The University of Maryland Electron Ring (UMER) (Invited), TOAA008, these proceedings.

[3] T. Godlove *et al*, The 10 keV Injector for the UMER Project, Proc. 1999 Particle Accel. Conf., 1970 (1999).

[4] S. Bernal *et al*, Transport of a Space-Charge Dominated Electron Beam in a Short-Quadrupole Channel, Phys. Rev. ST Accel. Beams 1, 044202 (1998).

[5] I. Haber *et al*, Computer Simulations of the UMER Electron Gun, RPAH045, these proceedings.

[6] W.W. Zhang *et al*, Design and Field Measurements of Printed-Circuit Quadrupoles and Dipoles, Phys. Rev. ST Accel. Beams 3, 122401 (2000).

[7] J. Harris *et al*, A Fast Beam Position Monitor for UMER, TPAH077, these proceedings.

[8] C.K. Allen *et al*, Optimal Transport of Low Energy Particle Beams, Proc. 1995 Particle Accel. Conf., 2324 (1996).

[9] H. Li *et al*, Printed-Circuit Magnets for the UMER- New Developments, TPPH060, these proceedings.